Available online at www.sciencedirect.com

ScienceDirect

journal homepage: www.elsevier.com/locate/jtte

Original Research Paper

The optimal shapes of piles in integral abutment bridges

Cheng Lan [a], *Bruno Briseghella* [b,*], *Luigi Fenu* [c], *Junqing Xue* [b], *Tobia Zordan* [a]

[a] *Bolina Ingegneria Ltd., Venezia 30174, Italy*
[b] *College of Civil Engineering, Fuzhou University, Fuzhou 350108, China*
[c] *Department of Civil Engineering, Environmental Engineering and Architecture, University of Cagliari, Cagliari 09124, Italy*

HIGHLIGHTS

- The horizontal stiffness of pile foundations in integral abutment bridges (IABs) has been investigated.
- A structural optimization technique is proposed to find the best solutions for pile foundations.
- The developed optimization method has been applied to a real 400 m-long IAB and a 500 m-long one.
- Different parameters have been analysed, including a) pinned or fixed pile head, b) pre-hole, c) pile diameter.

ARTICLE INFO

Article history:
Received 6 June 2017
Received in revised form
18 August 2017
Accepted 21 August 2017
Available online 21 November 2017

Keywords:
Integral abutment bridges
Structural optimization
Concrete piles
FEM simulation

ABSTRACT

Integral abutment bridges (IABs) can be used to avoid the durability issues associated with bearings and expansion joints. For this type of bridge, the design of the optimal pile foundation, especially with respect to the horizontal stiffness, is a challenging issue. A structural optimization approach is proposed in this paper to optimize the pile foundation shape in integral abutment bridges. A procedure was implemented based on linking MATLAB, where an optimization code was developed, and OpenSees, which was used as the finite element solver. The optimization technique was compared with other techniques developed in previous researches to verify its reliability; the technique was then applied to a real 400 m-long IAB building in Verona, Italy, as a case study. The following two possibilities were considered and compared: (a) a pile with two different diameters along the depth and (b) a pile with a pre-hole. In fact, to increase the lateral and rotational flexibilities of the pile head, piles for an integral abutment bridge foundation are often driven into pre-deep holes filled with loose sand. Finally, the case of super-long integral abutment bridges ($L = 500$ m) with a corresponding displacement on one bridge end of approximately 50 mm was analysed. The following four pile design optimization cases were considered with similar study criteria as the Isola della Scala Bridge: (a) a pinned pile head for semi-integral abutment, (b) a fixed pile head without a pre-hole, (c) a fixed pile head with a pre-hole of any depth, (d) a fixed pile head of a pre-hole with a depth limit (< 2 m) allowing for enough

* *Corresponding author*. Tel.: +86 591 22865378; fax: +86 591 22865378.
E-mail addresses: lan@bolinaingegneria.com (C. Lan), bruno@fzu.edu.cn (B. Briseghella), lfenu@unica.it (L. Fenu), junqing.xue@fzu.edu.cn (J. Xue), zordan@bolinaingegneria.com (T. Zordan).
Peer review under responsibility of Periodical Offices of Chang'an University.
https://doi.org/10.1016/j.jtte.2017.11.001

embedded length for the friction pile. The case studies confirmed the potential of the proposed optimization techniques for finding the optimal shape of piles in integral abutment bridges.

1. Introduction

Traditionally, expansion joints, roller supports, and other structural releases are used on bridges to prevent damage caused by superstructure expansion and contraction due to temperature variations, creep and shrinkage. Expansion joints and bearings increase the initial cost of a bridge and often do not function properly after years of service unless they are extensively maintained. Thus, integral abutment bridges (IABs), which have no expansion joints and bearings within the span or at the supports (Fiore et al., 2012, 2013), provide an alternative design (Briseghella and Zordan, 2015; Burke, 1993) that potentially offers lower initial costs and lower maintenance costs (Mahesh, 2005). IABs can be used for newly built bridges and to retrofit existing bridges (Briseghella and Zordan, 2007; Dong et al., 2014; Yannotti et al., 2005; Zordan and Briseghella, 2007). The monolithic connections between the deck and the sub-structure make IABs different from other conventional bridges and allows for a remarkably increased redundancy with improved response to seismic loading and other extreme events (Erhan and Dicleli, 2015; Xue et al., 2014; Zordan et al., 2011a). Furthermore, deck joints are known to be a continuing problem in existing bridges, due not only to their own failure and maintenance problems but also to the significant amount of corrosion damage in the girders and underlying substructures caused by run-off water containing corrosive de-icing salts leaking through the joints in the deck (Arockiasamy and Sivakumar, 2005). Presently, most European countries and U.S. states attempt to use IABs or semi-IABs for short-or medium-sized bridges (usually up to 100 m). The application of IABs based on their maximum length and the possibility to design super-long integral abutment bridges was investigated by several authors (Baptiste et al., 2011; Dicleli and Albhaisi, 2004; Zordan et al., 2011b).

However, soil-structure interaction problems due to thermal and long-term loads still represent a challenging issue requiring close cooperation between structural and geotechnical engineers.

According to several codes and guidelines for IABs, piles should be flexible under forces and moments acting on the abutment to settle horizontal movements, expansion and contraction induced by temperature variations, creep and shrinkage. Thus, the piles in IABs are often installed with their weak axis of bending resistance parallel to the bridge centreline (Greimann et al., 1987).

Design details for piles used in IABs were proposed in several studies (Franco, 1999). For example, studies completed in New York and Pennsylvania determined that piles should be designed for vertical and lateral loads; fixity between the superstructure and pile top is ignored. The Pennsylvania study also stated that piles should be analysed for bending induced by superstructure movements. Maine provided a step-by-step design procedure for piles. In North America, steel H-piles have typically been used in IABs to meet flexibility requirements, while in Europe and Asia, concrete piles are adopted (Gama and Almeida, 2014). Some states, such as Virginia, Pennsylvania and New York, allow the use of concrete encased-steel piles. Pennsylvania and New York specify that concrete encased piles shall not be used with spans greater than 150 feet (45.7 m). Virginia specifies the use of only concrete piles with a shelf abutment, similar to a spread footing on a set of piles. The majority of states in the U. S. specified orienting piles on their weak axis, perpendicular to the direction of movement (Wasserman, 2007). Two states specified using strong axis orientation, and other states had specific criteria for which orientation to use. For instance, New York related the use of axis to length of span (weak axis for spans less than 90 feet per 27.4 m, strong axis for spans greater than 90 feet per 27.4 m).

Typically the horizontal loads induced by the superstructure contraction and expansion are complicatedly distributed in the substructures due to the interactions of the soil-abutment and soil-pile (Burke Jr., 2009). The backfill earth pressure may take the larger proportion of the applied load (74%–88%), while the shear force at the top of the pile may take the small proportion (12%–26%) (Arsoy et al., 1999). This distribution might be caused by the geo-phenomenon of "ratcheting" (Horvath, 2004). Meanwhile, the displacement at the top of the pile nearly equals to the displacement at the top of the stub-type abutment. Therefore, the piles should be designed with the ability to accommodate a certain (lateral) shear force and large thermal-induced displacement.

Even if most codes indicate that flexible piles are better, it is not clear how to determine the optimal horizontal stiffness for a bridge and how to design the piles accordingly.

Therefore, a structural optimization tool to shape the piles used in integral abutment bridges according to the required flexibility is presented in this paper. The design optimization approach applied to find the optimal pile shapes is introduced in Section 2. The finite element (FE) modelling techniques used in the research and their verification based on previous research are described in Sections 3 and 4. In Section 5, a case study of an integral abutment bridge of 400 m built in Isola della Scala (Verona, Italy) is introduced, and the results are discussed. Finally, the conclusions are drawn in Section 6.

2. Design optimization approach

Structural optimization is an important tool for sizing structure members and for helping designers find the most suitable shape of a structure from the structural and architectural points of view (Adriaenssens et al., 2014; Briseghella et al., 2016; Fiore et al., 2016; Marano et al., 2014). Structural optimization is common in mechanical and aeronautical engineering, and in recent years, it has been progressively adopted for structural-engineering applications such as buildings and bridges (Allahdadian and Boroomand, 2010; Briseghella et al., 2013a,b; Greco et al., 2016; Greco and Marano, 2016; Huang and Xie, 2008; Neves et al., 1995; Quaranta et al., 2014; Stromberg et al., 2010; Zordan et al., 2010).

2.1. *Optimization problem description*

Generally, the independent variables in an optimization problem are the design variables (DV). The vector of the design variables is indicated by Eq. (1).

$$X = (X_1, X_2, \cdots, X_n) \tag{1}$$

The design variables are subject to n constraints with upper and lower limits, that is shown as Eq. (2).

$$\underline{X_i} \le X_i \le \overline{X_i} \quad i = 1, 2, \cdots, n \tag{2}$$

where n is number of design variables. The design variable constraints are often referred to as side constraints and define the feasible design space.

Now, minimize

$$f = f(X) \tag{3}$$

subject to

$$\begin{cases} g_i(X) \le \overline{g_i} & i = 1, 2, \cdots, m_1 \\ \underline{h_i} \le h_i(X) & i = 1, 2, \cdots, m_2 \\ \underline{w_i} \le w_i(X) \le \overline{w_i} & i = 1, 2, \cdots, m_3 \end{cases} \tag{4}$$

where f is objective function (OBJ); g_i, h_i, w_i are state variables (SV) containing the design, with under-bars and over-bars representing lower and upper bounds, respectively, called constraints function (CON); the sum of m_1, m_2, m_3 is the number of state variable constraint with various upper and lower limit values. The state variables can also be referred to as dependent variables in that they vary with the vector X of the design variables in forms of equations and in equations. The objective function in structural optimization is typically considered as a function of the design variables that have to be minimized (or maximized) when the optimum design solution is found. For instance, considering stress level in a certain structure region as an objective function, the deflection in a certain point, the total volume (or weight) in this latter case deflection and the stress are usually chosen as state variables to control the behaviour of the structure during the optimization procedure.

Design configurations with certain design variable values that satisfy all constraints are referred to as feasible designs. Design configurations with one or more violations are termed infeasible. In defining a feasible design space, a tolerance is added to each state variable limit.

As design sets are generated by methods or tools (e.g., the subproblem approximation method) and after an objective function is defined, the best design set is computed and its number is stored. The best set is determined if one or more feasible sets exists, and the best design set is the feasible set with the lowest objective function value. In other words, the best set is that which most closely agrees with the mathematical goals expressed.

For example, in the case analysed in this paper, the pile to be optimized consists of two different sections with a circular solid section of reinforced concrete as shown in Fig. 1. The design purpose is to minimize the top displacement of the pile.

The design problem to be solved is which diameter and length of upper and lower pile sections minimize the top displacement for a given pile volume and an assigned magnitude of the horizontal force applied at the top. Then, this optimization problem can be described as follows:

- Design variables (DV): section diameters D_1, D_2 and lengths L_1, L_2;
- Constraint function (SV/CON): pile bending moment, M < MR, with MR pile bending resistance or concrete stresses $\sigma_c < f_{ck}$, with f_{ck} concrete characteristic compressive strength, and reinforcement stresses, $\sigma_s < f_{yd}$ with f_{yd}

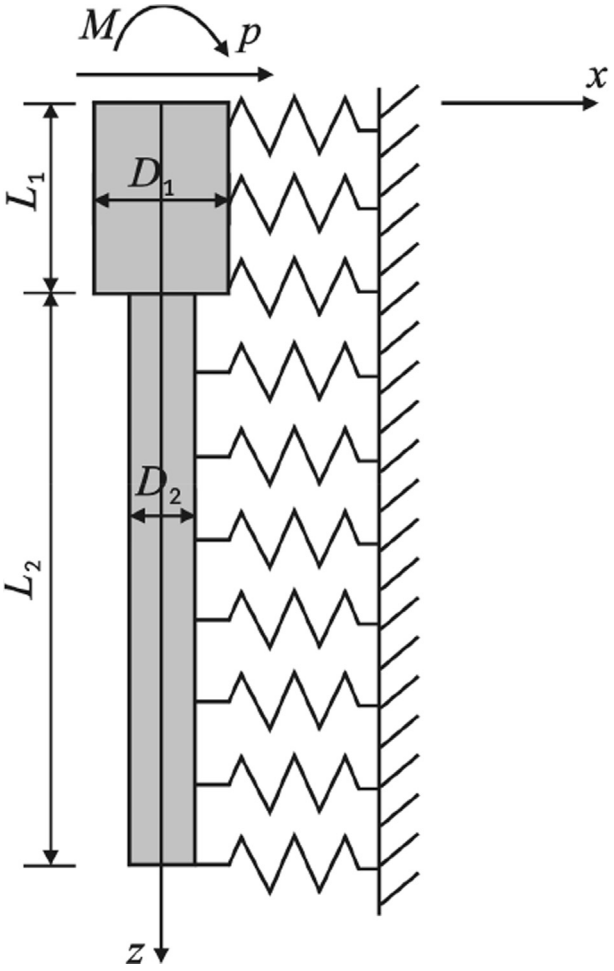

Fig. 1 – Model of the R/C bored pile made up of two parts.

design stress for reinforcement; maintaining the same total volume of material V_{tot} = const.
- Objective function (OBJ): pile head displacement v_0.

2.2. *Optimization procedure*

In this paper, a procedure based on linking MATLAB (MathWorks Inc., 2011), where a code for optimization was developed, and OpenSees (OpenSees, 2011), is used as a finite element solver, was implemented, as shown in the flowchart in Fig. 2. The advantages of modelling by finite elements in OpenSees will be illustrated in the next section.

In MATLAB, the method of the coupled local minimizers (CLM) was used. CLM is a recently developed global optimization technique in which the information of several local optimizers is combined to avoid local optima (MathWorks Inc., 2011; Suykens et al., 2001; Teughels et al., 2003). The local optimizations are started from random points over the domain, and constraints are imposed to force the search points to end in the same point. In a successful run, this point has the lowest function value and is the global minimum. The reliability of this method is due to the evaluation of many points spread over the domain. The advantage compared to other global methods is the use of first order information, which enforces faster convergence. To reduce calculation time, this method is used to identify the global minimum with limited precision. When the search points have located the valley of the global minimum, the CLM-method is stopped and a local method (a trust region method in which derivative information is used to compute a good approximation of the objective function in a small trust region or a least squares technique) is used until the necessary precision is reached.

Initially in this procedure, based on the optimization description, the design variables were assigned. Then, their values were written to a file and passed to subroutines that compute the objective function and constraint function, where the finite element modelling and solving part might be called according to the objective and constraint required.

Based on these loops of creating design variables (DV), calculating constraints (SV/CON) and objectives (OBJ), the optimization problem sampling was passed to the "global optimization" setup. Then, by setting global search control parameters (such as variables tolerances, maximum iteration

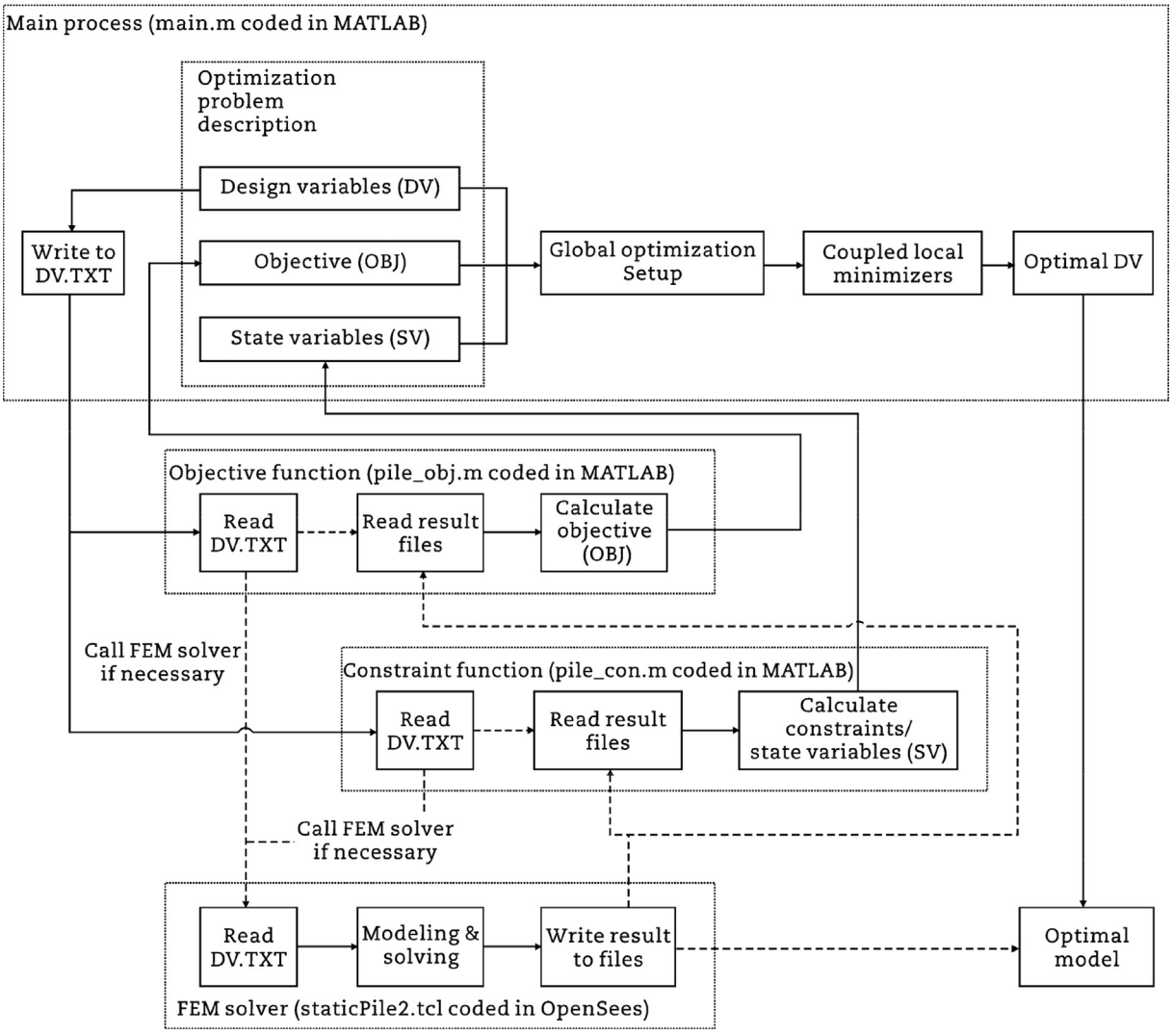

Fig. 2 – Flowchart of the developed optimization procedure.

number and search step size), coupled local minimizers were launched until either the converged optimal solution was found or convergence was not achieved if the tolerances were not respected or maximum iteration numbers were reached.

3. Finite element modelling of pile

David and Forth (2011) demonstrated six modelling approaches used to consider soil-structure interactions as follows.

1) Winkler spring approach: the field elimination method where the soil media is represented by a spring element.
2) Finite element analysis: a monolithic approach.
3) Integrated modelling: a finite element approach also known as a coupled soil-structure interaction system accounting for interface elements.
4) Partitioned analysis: two elements are analysed as isolated entities.
5) Staggered approach: two physically partitioned and independent domains represent both soil and structure, respectively, also known to be suited to transient dynamic analysis only.
6) Iterative coupling: a similar modelling approach as the staggered approach but with parallel computing.

Regarding the design method, the most common method used in design of IABs is the *p*-*y* method. In this method, the three-dimensional (3D) laterally loaded pile problem is analysed by using a beam on a nonlinear Winkler foundation (BNWF) in which uncoupled one-dimensional (1D) springs are used to describe the soil-pile interaction. Therefore, despite known shortcomings inherent to the method, the *p*-*y* approach can be used successfully in many types of lateral pile analysis. Finite element simulations were conducted using the open-source FE framework of OpenSees. Embedded in this open-source software, the soil materials models are based on API recommendation and fibre sections are available for building pile concrete sections (American Petroleum Institute, 2000). Furthermore, the important advantage of OpenSees is that it can easily interact and exchange data with MATLAB through file operations during the optimization process.

The model was adapted starting from a simple example of OpenSees-a beam on a nonlinear Winkler foundation (BNWF) (McGann and Arduino, 2011; McGann et al., 2011) and was developed by applying a fibre section and non-linear materials properties. In the optimization example of the pile design of integral abutment bridges developed in Section 5, the pile of Isola della Scala Bridge was taken from the global model. The forces obtained on the pile head were applied as the loads on pile; the same soil condition was considered, and the geometry and section properties were all taken as starting values for optimization. In the model of the laterally loaded pile problem, displacement-based beam elements were used to represent the pile, and a series of nonlinear springs were used to represent the soil. The soil springs were generated using zero-length elements assigned to separate uniaxial material objects in the lateral and vertical directions. An idealized scheme of the laterally loaded pile model is provided in Fig. 3.

3.1. *Spring constitutive behaviour*

The constitutive behaviour of the springs was defined such that the springs oriented in the lateral direction represent *p*-*y* springs, and the vertically oriented springs represent *t*-*z* and *Q*-*z* springs for the pile shaft and tip, respectively. Zero-length elements were used for the soil springs using the element zero-length. These elements connected the fixed and slave spring nodes. The *p*-*y*-Simple1 material objects were incorporated in the *x*-direction (direction of loading), while the *Q*-*z*-Simple1 and *t*-*z*-Simple1 material objects were incorporated in the *z*-direction (vertical direction) at the pile tip and along the shaft, respectively.

The equations describing the *p*-*y*-Simple1 behaviour were described as the backbone of the *p*-*y* curve by approximating the Matlock (1970) soft clay relation (when soil Type is 1), while the backbone of the *p*-*y* curve approximates the API sand relation (when soilType is 2) (Boulanger et al., 1999). Similarly, *t*-*z*-Simple1 material was defined as the backbone of the *t*-*z* curve by approximating Reese and O'Neill (1987) (when soilType is 1) while the backbone of the *t*-*z* curve approximates the Mosher (1984) relation (when soilType is 2). Additionally, *Q*-*z*-Simple1 was implemented as the backbone of the *Q*-*z* curve by approximating the relation determined by Reese and O'Neill (1987) for drilled shafts in clay (when *Q*-*z*-Type is 1) while the backbone of the *Q*-*z* curve approximates the relation determined by Vijayvergiya (1977) for piles in sand (when *Q*-*z*-Type is 2).

The constitutive behaviours of these uniaxial material objects automatically generate the required spring material objects based upon the input geometry and soil properties in the modelling input file.

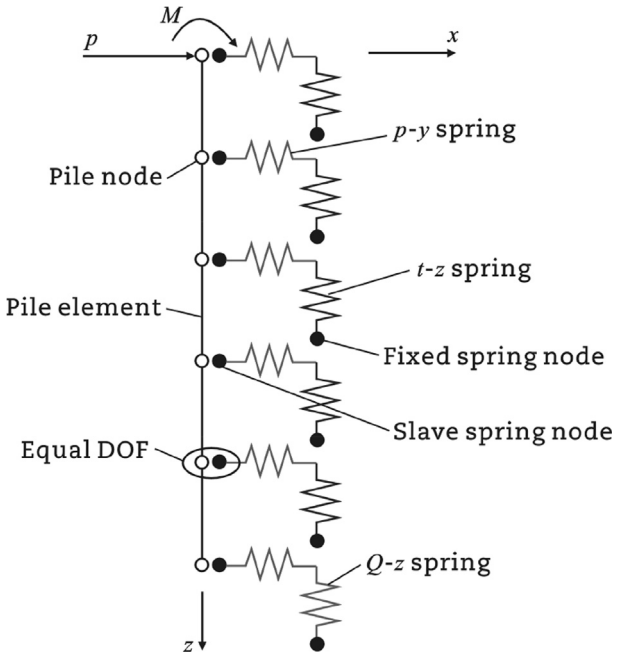

Fig. 3 – Pile model in OpenSees.

3.2. *Pile constitutive behaviour and element*

The displacement-based beam element, element dispBeamColumn, which is based on the displacement formulation and considers the spread of plasticity along the element, was used to facilitate the incorporation of the elastoplastic pile section behaviour using fibre section models. A fibre section has a general geometric configuration formed by sub regions of simpler, regular shapes (e.g., quadrilateral, circular and triangular regions). In addition, layers of reinforcement bars can be specified. Individual fibres, however, it can also be defined and associated with uniaxial Material objects, which enforce Bernoulli beam assumptions. In this model, uniaxial Material Steel02, a uniaxial Menegotto-Pinto (1973) steel material object with isotropic strain hardening, was used for reinforcement; uniaxial Material Concrete02, a uniaxial concrete material object with tensile strength and linear tension softening (a Fedeas material), was used for confined and unconfined concrete. The geometric parameters are defined with respect to a planar local coordinate system (y, z), as shown in Fig. 4.

The pile nodes over the embedded length of the pile are linked with the slave spring nodes (using the equal DOF command). The pile nodes are the master nodes in this example. These two sets of nodes share equal degrees-of-freedom in the x- and z-translational directions only.

4. Verification with previous research

To verify the adopted modelling and optimization techniques, a case study of a R/C bored pile laterally loaded at the top by a force $p = 100$ kN ($M = 0$, considering a pin connection between pile-abutment) developed by previous researchers (Fenu and Madama, 2006) was considered. The unitary coefficient of the subgrade reaction of the earth was $k_h = 11.1$ MPa, referred to as a cohesive soil with undrained cohesion $c_u = 0.166$ MPa. The Young's modulus of the concrete was $E_c = 25{,}000$ MPa. The parameter values (linear materials) were the same as those in the design example presented by Fenu and Madama, where an exhaustive enumeration search was used to determine the optimal solution instead of using a global optimization algorithm.

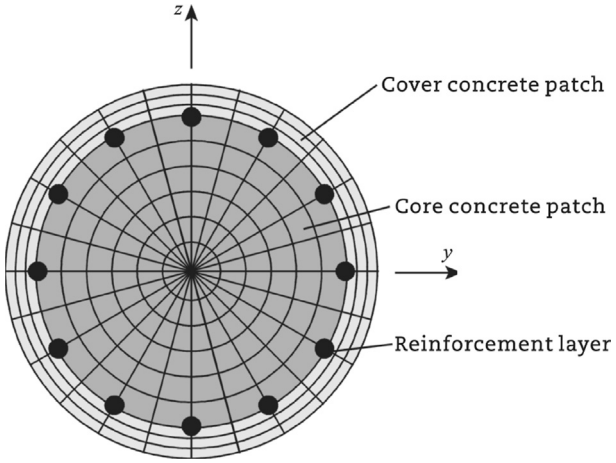

Fig. 4 – Example of fibre section of reinforced concrete.

The lateral loaded pile, usually considered as surrounded by Winkler soil, is widely designed and used in many structures (Fenu and Serra, 1995). Therefore, as a design optimization problem, a pile with changing diameter was implemented through the finite element method; its top displacement was minimized by varying the design variables that are the dimensions of each of the two pile parts needed to describe it.

This optimization problem can be described by defining design variables, state variables (constraints) and objectives; the initial values and optimization ranges are listed in Table 1. The pile total volume of 2 m^3 is assigned. The procedure started from a pile with a uniform section of diameter of 0.6 m (Fig. 5).

The converged results obtained through the optimization procedure are shown in Fig. 6. The optimum pile made up of two parts with two different diameters has an upper part with $D_1 = 1.305$ m and $L_1 = 0.79$ m, and the lower part with $D_2 = 0.500$ m and $L_2 = 4.79$ m. This result is validated by the same optimum solution found by an exhaustive enumeration search by Fenu (optimal discrete variables $L_1 = 0.8$ m, $L_2 = 4.8$ m, $D_1 = 1.3$ m, $D_2 = 0.5$ m). This optimization procedure was also verified with the solutions of different section types, like a hollow circular section, and different pile parts, as the optimum solutions already obtained by Fenu and Madama.

Therefore, in the next section, the same optimization procedure is applied in a different design problem with different modelling conditions to determine the optimal pile profile for an integral abutment bridge.

5. Case studies

This case study concerns a flyover completed in 2007 at Isola della Scala in Verona, Italy (Zordan et al., 2011a). The total length of the structure, arranged on 13 spans, is approximately 400 m. The construction of the bridge, which began in 2001 as a simple supported flyover, was halted after 2 years because of economic problems affecting the contractor. At that time, all prestressed concrete girders and the main pre-fabricated elements were nevertheless purchased. In the early 2006, work resumed with a new proposal that aimed to improve the quality of the structure and change the static scheme from "simply supported" to "fully integral", without modifying the already built foundations and piers. The elevation layout is shown in Fig. 7. Details of the typical cross section are given in Fig. 8. The piles arrangements are shown in Fig. 9, and the pile properties are given in Table 2.

5.1. *Optimized design of pile shape*

When studying laterally loaded piles, the results obtained using a surrounded Winkler's soil are generally comparable to those obtained through a continuous elastic semi-space model, even when (as in many real cases) the length of the piles is long and penetrates several soil layers whose

Table 1 – Optimization problem of lateral loaded pile.s

Problem description	Parameter	Initial value	Limit	Optimal value
Design variable	Length of part 1, L_1 (m)	1.000	0.5–2.0	0.790
	Length of part 2, L_2 (m)	6.100	4.0–8.0	4.790
	Diameter of part 1, D_1 (m)	0.600	0.5–1.5	1.305
	Diameter of part 2, D_2 (m)	0.600	0.5–1.0	0.500
State variable/constraint	Total volume, V_{tot} (m^3)	2.000	Difference < 0.5%	1.997
Objective	Displacement of pile head, d_0 (mm)	10.3	Minimum	8.3

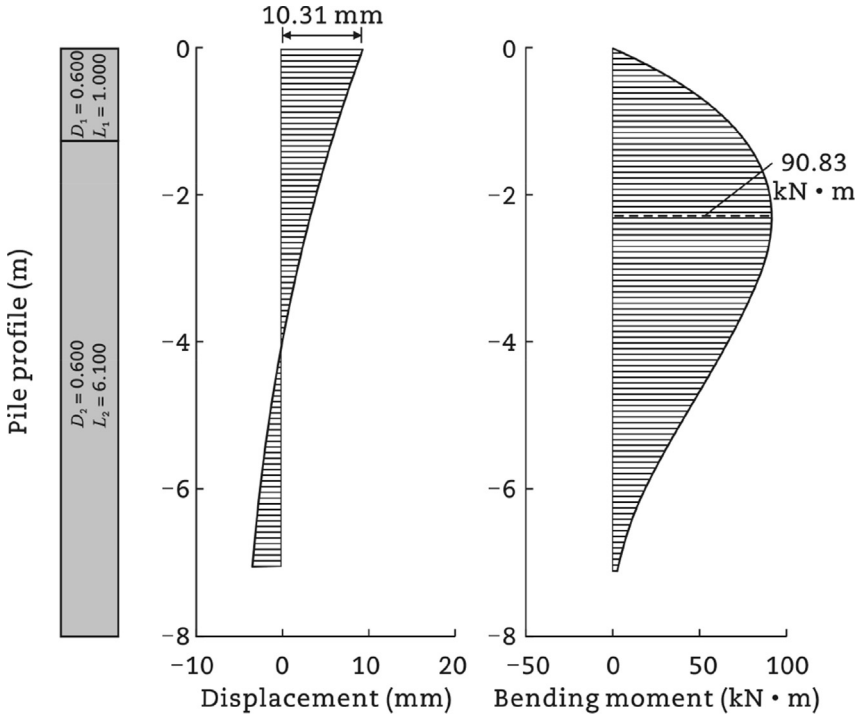

Fig. 5 – Stating profile of lateral loaded pile.

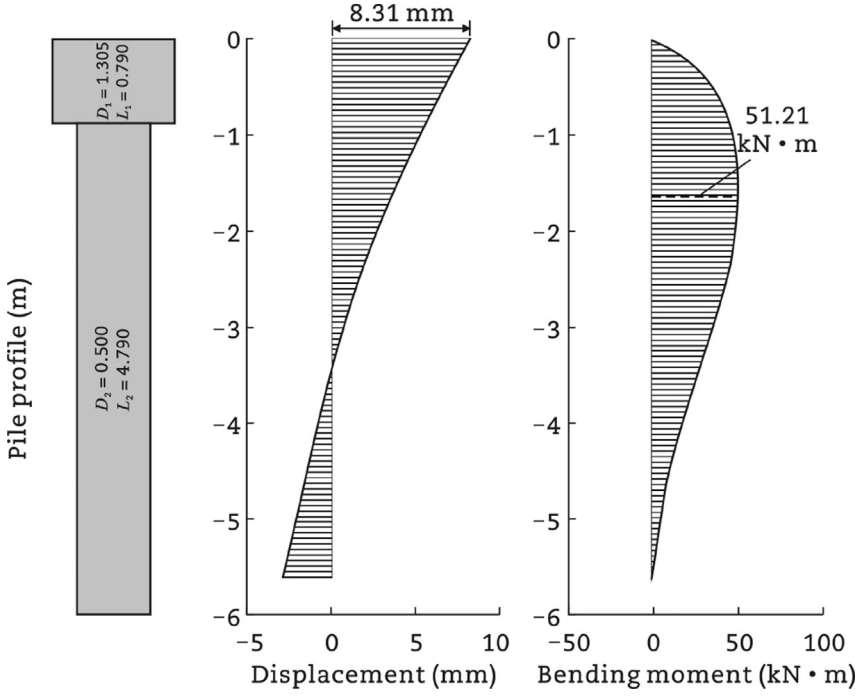

Fig. 6 – Optimized profile of lateral loaded R/C pile.

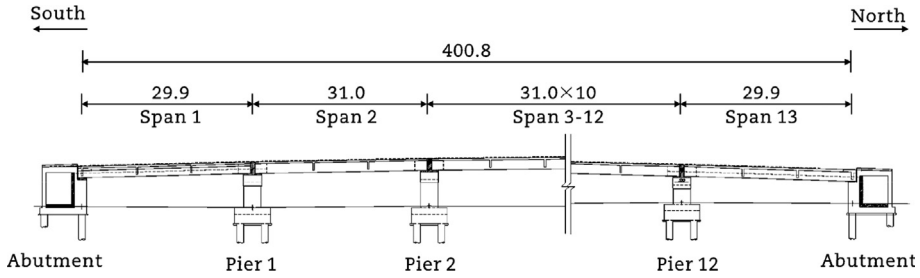

Fig. 7 – Elevation layout of Isola della Scala Bridge (m).

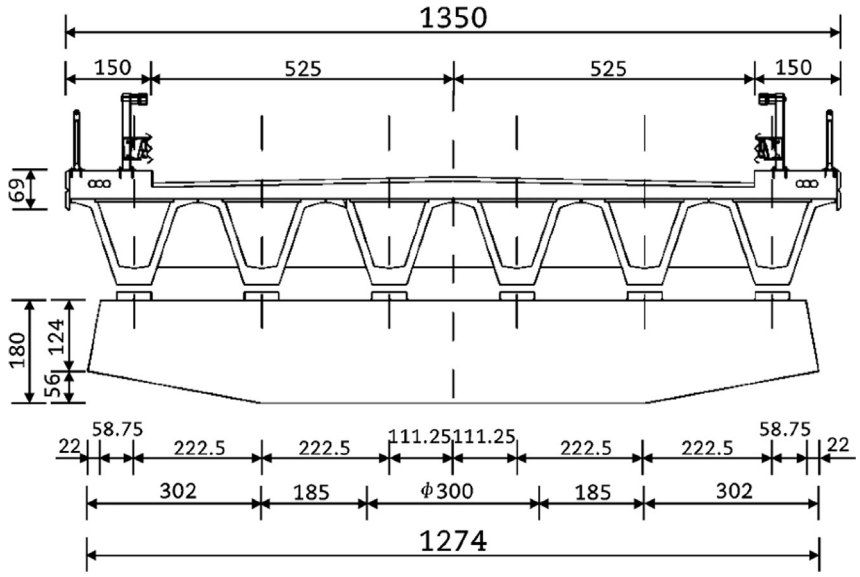

Fig. 8 – Typical cross section of Isola della Scala Bridge (cm).

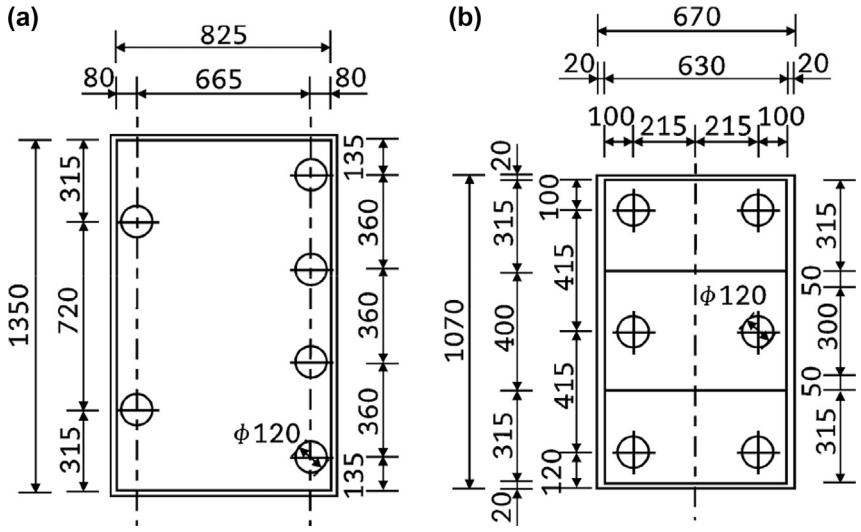

Fig. 9 – Plan view of piles arrangement at abutments and pier footings (cm). (a) South abutment (symmetric in north). (b) Pier footing.

subgrade reaction can vary significantly between the different layers and along each layer, thus varying with depth. Moreover, in integral abutment bridges, large thermal induced displacement would appear and lead to the yielding of soils, so that the behaviour of the soil springs and pile sections becomes nonlinear. Therefore, by implementing the pile model for an integral abutment bridge, real soil conditions and non-linear material properties along the pile were considered following the pile modelling conditions allowed by OpenSees.

Table 2 – Pile properties of the Isola della Scala Bridge.

	Beneath abutment	Beneath pier footing
Material	Concrete C35/40	Concrete C35/40
Reinforcement	30ϕ26 mm with cover of 40 mm	30ϕ26 mm with cover of 40 mm
Type	Friction	Friction
Numbers	4 + 2	3 × 2
Section shape	Circular	Circular
Diameter (m)	1.20	1.20
Length (m)	15	20

5.2. *Pile size limits considering ultimate axial load*

To perform pile design optimization, the loading and boundary conditions of the piles of the Isola della Scala Bridge were taken as example. Considered as a friction pile, the total length of the pile was constrained to an original length of 15 m to have enough friction length for the pile. From the full bridge model analyses, the maximum axial load on the pile was approximately 2000 kN. Therefore, a lower size bound of the pile with respect to this length and the axial load were required. According to the Rankine equation and the circular concrete section resistances, the ultimate load, N_u, can be expressed as the following Eq. (5) (Greimann et al., 1987).

$$\frac{1}{N_u}=\frac{1}{N_{cr}}+\frac{1}{N_{pl}} \tag{5}$$

where N_{cr} is elastic buckling load, N_{pl} is plastic capacity as calculated according to Table 3, k_h is the initial stiffness of the soil, E and I are the elastic modulus and moment of inertia of the pile, n_h is constant of subgrade reaction ($n_h = k_h/z$), N_p, M_p are section resistances as estimated through Eqs. (6) and (7), d_0 is displacement of pile head (assuming a large displacement of d_0 is 50 mm).

$$N_p=\alpha f_{cd}A\left(1-\frac{\sin(2\pi\alpha)}{2\pi\alpha}\right)+(\alpha-\alpha_t)f_{yd}A_s \tag{6}$$

$$M_p\approx\frac{1}{3}f_{cd}AD\frac{\sin^3(\pi\alpha)}{\pi}+f_{yd}A_s\left(\frac{D}{2}-a\right)\frac{\sin(\pi\alpha)+\sin(\pi\alpha_t)}{\pi} \tag{7}$$

where α is compression concrete central angle ratio (assuming compression area of half section, α is 0.5), α_t is tension reinforcement ratio ($\alpha_t = 1.25 - 2\alpha$, when $\alpha < 0.625$), a is concrete cover thickness (a = 0.04 m), A is section area, A_s is reinforcement area (assuming A_s/A = 1.5%), D is section diameter, f_{cd} is concrete design strength, f_{yd} is reinforcement design strength. By these assumed values and the conservative buckling consideration of soft clay soil with k_h = 1.742 MPa, it was found that the governing factor for this pile was the plastic capacity N_p. The resulting ultimate loads are plotted in Fig. 10.

Therefore, for the axial plastic capability and stability considerations for a length of 15 m under the maximum equivalent axial load of approximately 2000 kN, the lower pile diameter bound was set as 0.5 m, and the vertical load was ignored during the optimization calculations.

5.3. *Pile optimization for Isola della Scala Bridge*

The pile was modelled as the substructure of a previous model used in designing the piles of the Isola della Scala Bridge. The loads were considered as a lateral force load of 857 kN (in the x-direction) and a bending moment of 358 kN·m (in the y-direction), applied at the head of the pile (uppermost pile node); because the axial compression increased the section resistance, the axial load was neglected. The surrounding soil properties are listed in Table 4. The pile to be optimized was made with circular solid sections of concrete with a reinforcement ratio of 1.5%, a cover thickness of 40 mm, and an initial section diameter of $D_1 = D_2$ = 1.2 m; the initial pile lengths were L_1 = 5 m, L_2 = 10 m, as shown in Table 5 and Fig. 11.

The converged result was obtained through the optimization procedure described above. The optimal pile profile is shown in Fig. 12. Under the same loads, the optimized pile was more flexible, with a larger top displacement and a volume reduction from 16.965 m^3 to 8.209 m^3, at nearly 50%. Additionally, the stresses in both the concrete and reinforcement were well controlled as setting limits. Considering the long-term effects, these limits might be set with a reduction factor, thus resulting a conservative solution for service state with lower loads. However, in this

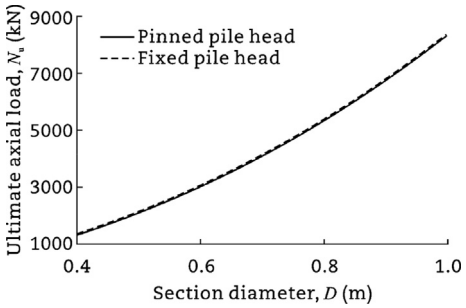

Fig. 10 – Ultimate loads referring to different section diameters.

Table 3 – Calculation formulae for axial capacity of pile (Greimann et al., 1986).

Capacity	Pinned pile head	Fixed pile head
Elastic buckling load, N_{cr}		
Constant soil stiffness	$2.0\sqrt{k_h EI}$	$2.5\sqrt{k_h EI}$
Linearly varying soil stiffness	$2.3(EI)^{\frac{3}{5}}(n_h)^{\frac{2}{5}}$	$4.2(EI)^{\frac{3}{7}}(n_h)^{\frac{2}{5}}$
Plastic capacity, N_{pl}		
Lateral deflection effect	$\frac{2M_p}{d_0}$ ($\leq N_p$)	$\frac{4M_p}{d_0}$ ($\leq N_p$)

Table 4 – Soil properties for piles in integral abutment bridge.

Depth (m)	Soil type	γ (kN/m^3)	φ (°)	c_u (kN/m^3)	With free water
0–−2.8	Sand	18.5	33	–	no
−2.8–−4.6	Sand	18.5	33	–	yes
−4.6–−6.8	Clay	18.5	–	26	yes
−6.8–−25.0	Sand	18.5	30	–	yes

Table 5 – Optimization problem of pile in integral abutment bridge.

Problem description	Parameter	Initial value	Limit	Optimal value
Design variable	Length of part 1, L_1 (m)	5.000	1.0–8.0	7.169
	Length of part 2, L_2 (m)	10.000	5.0–15.0	7.831
	Diameter of part 1, D_1 (m)	1.200	1.0–2.0	1.088
	Diameter of part 2, D_2 (m)	1.200	0.5–1.5	0.501
State variable/constraint	Total length, $L_1 + L_2$ (m)	15.0	Difference < 5%	15.0
	Stress in concrete, σ_c (MPa)	13.09	<30	19.42
	Stress in reinforcement, σ_s (MPa)	195.56	<330	329.94
Objective	Total volume, V_{tot} (m^3)	16.965	Minimum	8.209

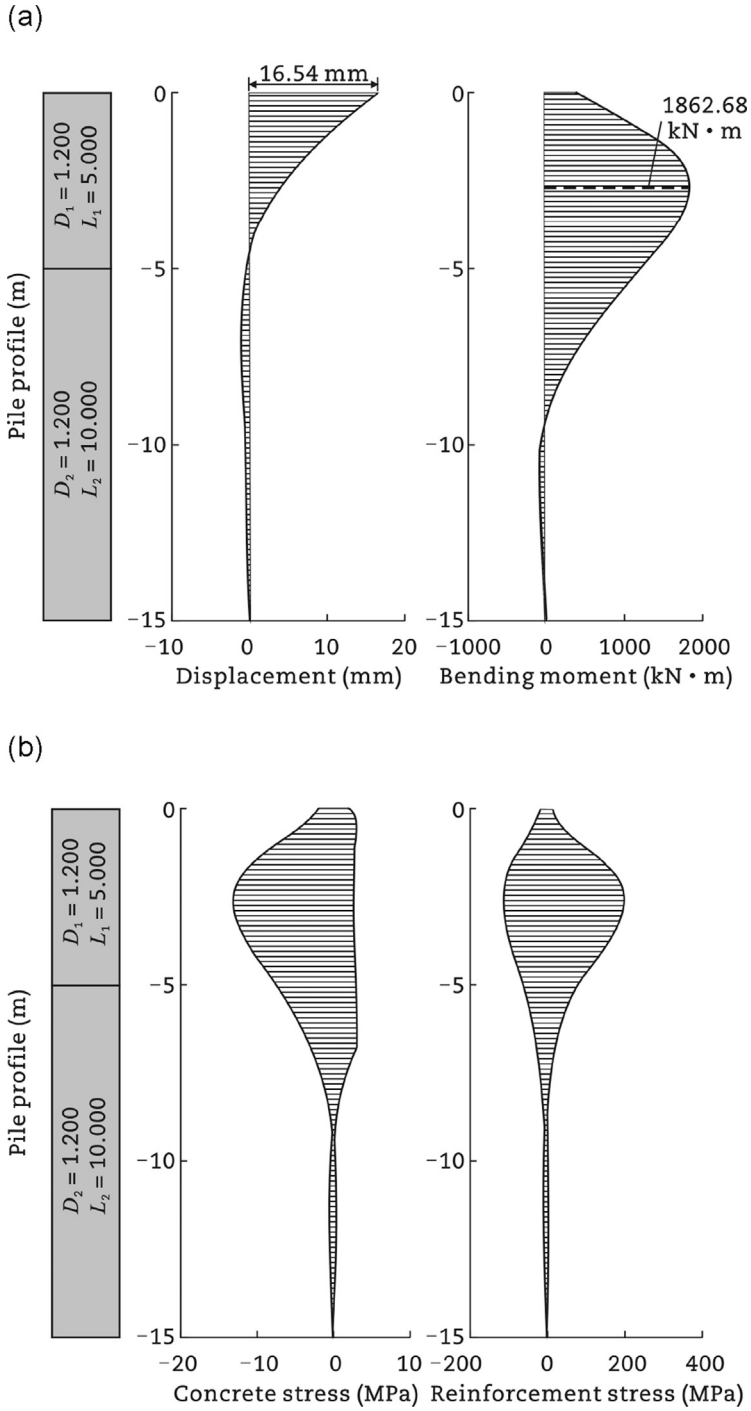

Fig. 11 – Original profile of R/C pile in integral abutment bridge. (a) Displacement and bending moment. (b) Stresses in concrete and reinforcement (positive and negative).

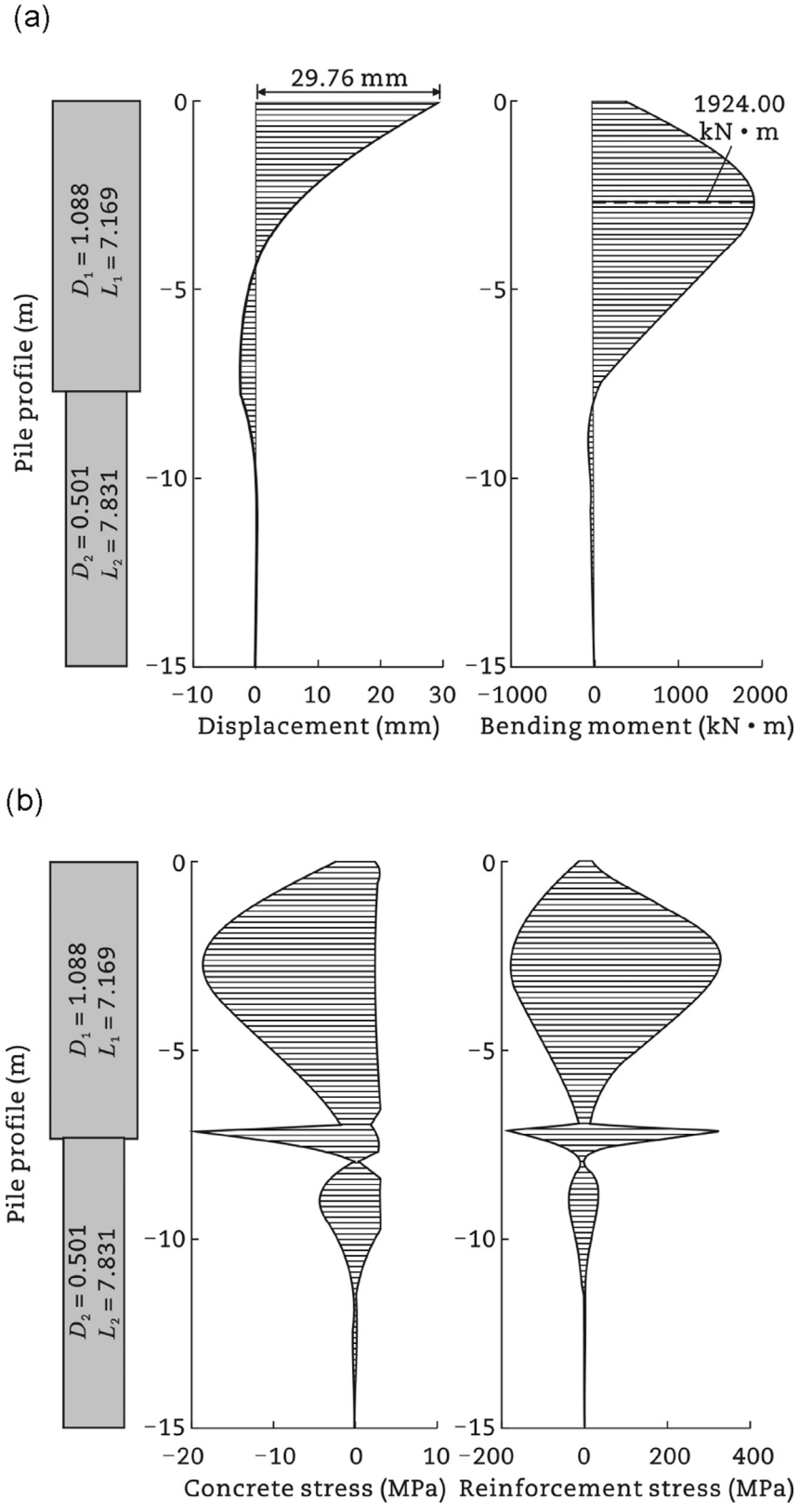

Fig. 12 – Optimized profile of R/C pile in integral abutment bridge. (a) Displacement and bending moment. (b) Stresses in concrete and reinforcement (positive and negative).

Table 6 – Optimization problem of pile with pre-hole.

Problem description	Parameter	Initial value	Limit	Optimal value
Design variable	Length of part 1 (pre-hole depth), L_1 (m)	2.000	0.2–5.0	0.225
	Length of part 2 (embedded part), L_2 (m)	13.000	5.0–15.0	14.775
	Diameter of pile, D (m)	1.200	0.8–1.2	1.031
State variable/constraint	Total length, $L_1 + L_2$ (m)	15.0	Difference < 5%	15.0
	Stress in concrete, σ_c (MPa)	18.34	<30	21.31
	Stress in reinforcement, σ_s (MPa)	249.67	<330	329.02
Objective	Total volume, V_{tot} (m^3)	16.965	Minimum	12.523

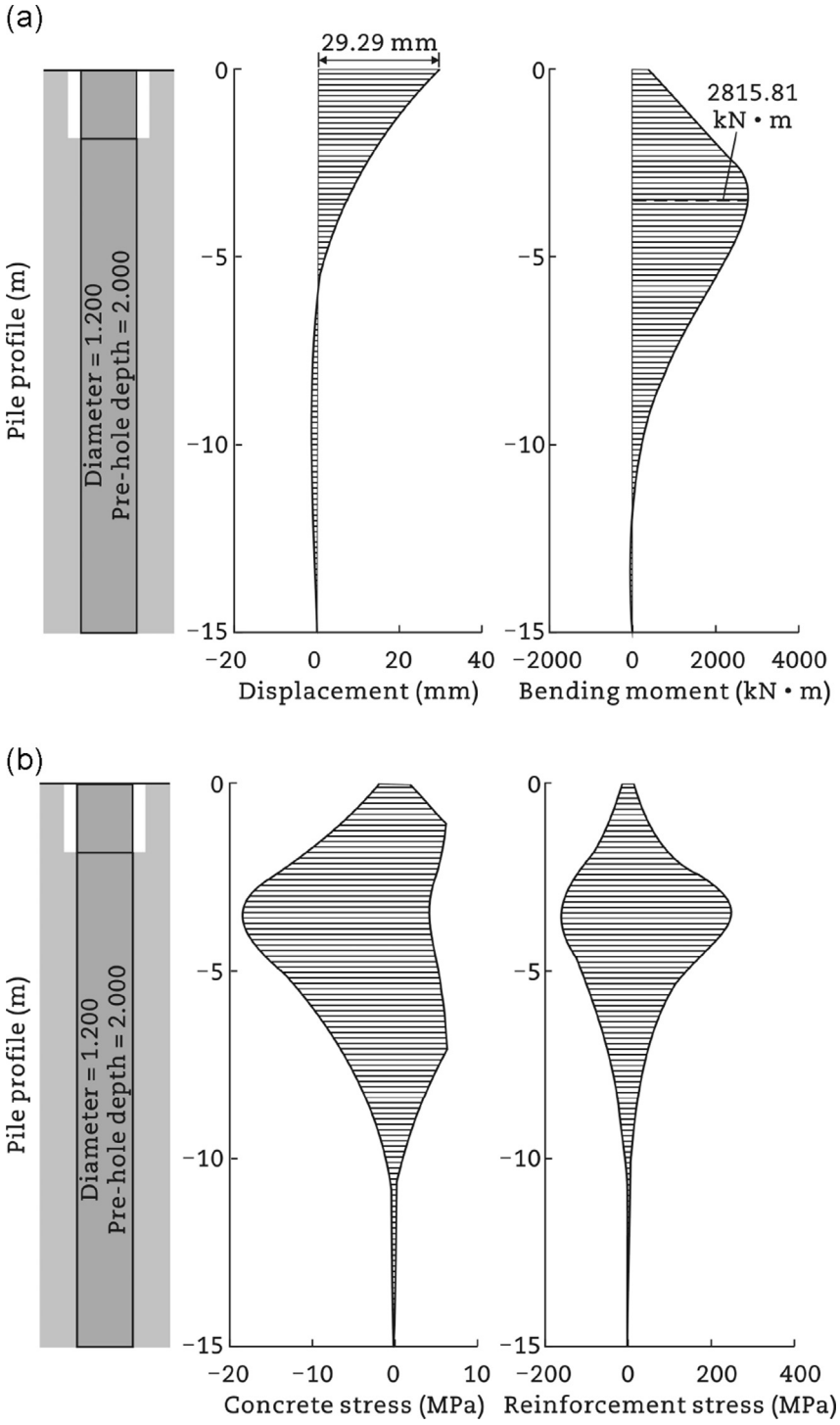

Fig. 13 – Starting profile of R/C pile with pre-hole. (a) Displacement and bending moment. (b) Stresses in concrete and reinforcement (positive and negative).

case study, the loads were taken from the ultimate state condition, which could be thought as more conservative.

In addition to fixing the reinforcement ratio, some pile designers prefer to vary the reinforcement ratio instead of the section diameter. However, the problem would be essentially the same. Through the optimization procedure presented herein, the optimal reinforcement ratio distribution was found to guide the design. However, to create these types of multi-section piles, efficient connections between different parts are necessary, which could make the construction more complicated and increase the time, technology, and cost to complete the work. Because the filling piles and prefabricated piles of the uniform section are widely used in engineering practice, it is worth optimizing the uniform diameter pile. In this case, the number of design variables is reduced in a more effective optimization procedure, as discussed in the next section.

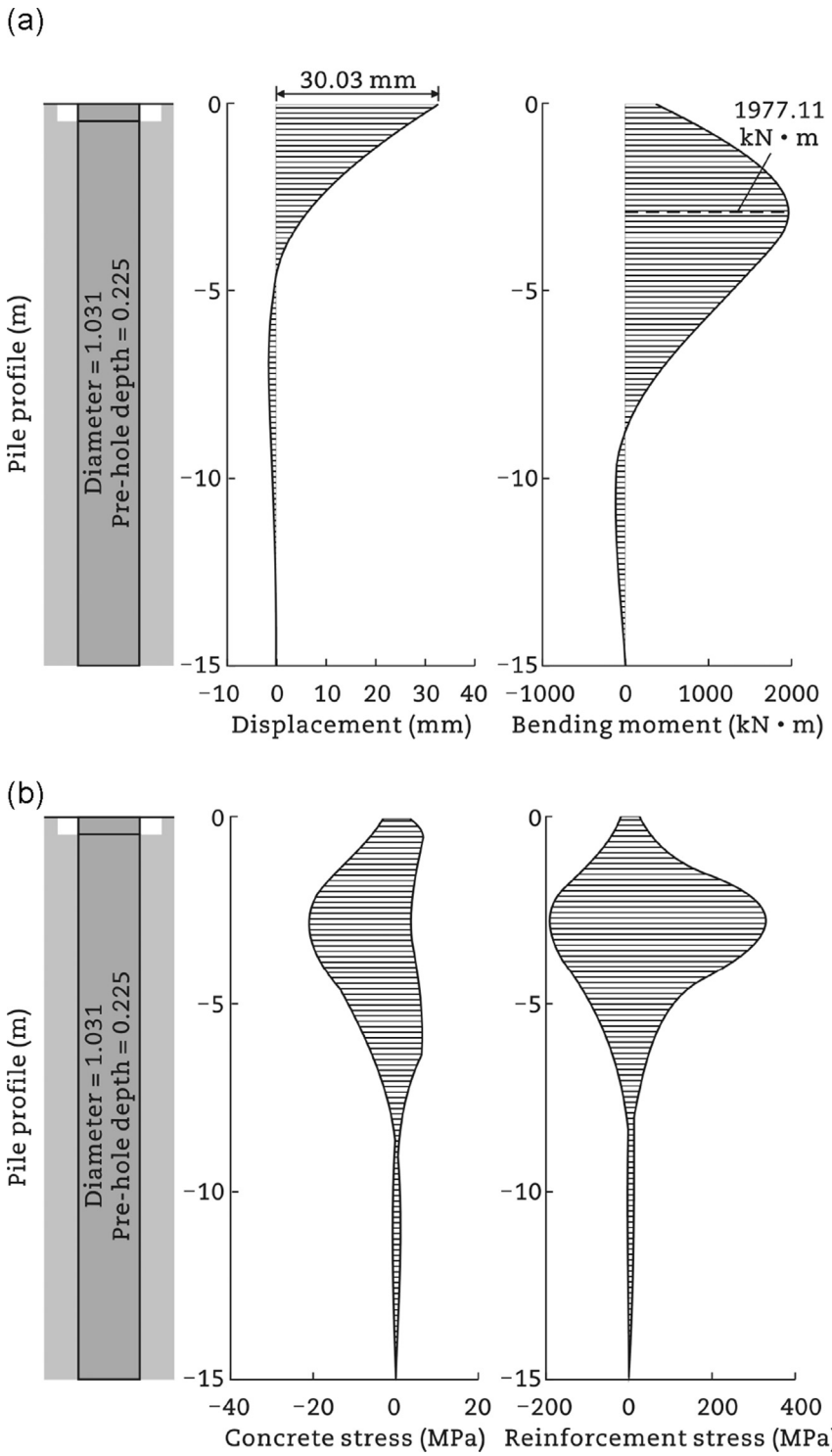

Fig. 14 – Optimized profile of R/C pile with pre-hole. (a) Displacement and bending moment. (b) Stresses in concrete and reinforcement (positive and negative).

Table 7 – Comparison of optimized piles.

Parameter	Initial value	Optimal with two sections	Optimal with pre-hole
Profile			
Length of part 1, L_1 (m)	5.000	7.169	0.225
Length of part 2, L_2 (m)	10.000	7.831	14.775
Diameter of part 1, D_1 (m)	1.200	1.088	1.031
Diameter of part 2, D_2 (m)	1.200	0.501	1.031
Total length, $L_1 + L_2$ (m)	15.000	15.000	15.000
Total volume, V_{tot} (m^3)	16.965	8.209	12.523
Δ (%)		−51.61	−26.18
Structural behaviour			
Pile head displacement, d_0 (mm)	16.48	29.78	30.03
Δ (%)		+80.70	+82.22
Maximum bending moment, M_{max} (kN·m)	1862.72	1924.00	1977.11
Δ (%)		+3.29	+6.14
Maximum stress in concrete, σ_c (MPa)	13.09	19.42	21.31
Δ (%)		+48.36	+62.80
Maximum stress in reinforcement, σ_s (MPa)	195.56	329.94	329.02
Δ (%)		+68.72	+68.25

5.4. *Pre-hole effects on pile design*

For integral abutment bridges, it is commonly thought that a foundation that is rotationally and translationally stiff results in larger superstructure loads during thermal loading. To increase the lateral and rotational flexibility of the pile head, the piles of an integral abutment bridge foundation are often driven into pre-augered (or pre-drilled) holes that are then backfilled with loose sand (Wasserman, 2007). Drilling a pilot hole for some top portion of a pile and then backfilling the hole with some type of loose backfill material creates a hinge-effect in the substructure. This increases the flexibility of the piles and of the substructure. Massachusetts guidelines specify pre-augering to a depth of 5 feet (1.5 m); other guidelines in New York specify a depth of 8 feet (2.4 m), while Pennsylvania and Maine specify a depth of 10 feet (3.0 m). New York suggests backfilling holes with sand; Massachusetts suggests backfilling with pea stone gravel, and Maine suggest using dense gravel. It has been shown that piles in 9 feet (2.7 m) deep predrilled holes filled with loose sand have a significant reduction in the equivalent stress and pile displacement (Thanasattayawibul, 2006).

This technique reduces stress concentration and increases deformations in the pile head thus improving pile durability, so the shape optimization of pre-holes has been performed. Considering the same optimization problem stated above and taking into account the convenience of fabrication and casting, the pile under consideration had a uniform section along its length, with a section of circular solid diameter of 1.2 m, a reinforcement ratio of 1.5% and a cover concrete of 40 mm. The starting profile is shown in Fig. 12. The optimization problem can be described as shown in Table 6.

The starting profile is shown in Fig. 13, and the optimal solution resulting from the optimization procedure is shown in Fig. 14. Comparing to the starting profile, the optimized solution had a smaller diameter and a shallow pre-hole depth yet few increments in flexibility (the limited displacement increment). Compared with the optimized profile as shown in Fig. 12, the flexibilities of these three solutions are at the same level; the optimal profile without pre-holes reaches the least volume expense (reduction of 50%), and the pile of the uniform section has less volume reduction (reduction of 25%) and a shallow pre-hole. Therefore, for economical piles, designers need to balance the savings between volume reduction and multi-section casting, according to the specific field conditions.

5.5. *Comparison of optimized piles*

Table 7 lists the optimized pile profiles, that is the profile with two varying sections, the profile with a uniform section and that with pre-hole treatment, together with their performance. Under the ultimate conditions occurring on the Isola della Scala Bridge, the proposed design optimization procedure designs piles with less resisting material and more displacement capacity. Although the stress level increases, these solutions are in an acceptable range. The two different

Table 8 – Optimized piles for imposed lateral displacement of 50 mm.

Parameter	Pinned pile head (no pre-hole)	Fixed pile head		
		No pre-hole	Pre-hole of any depth	Pre-hole of limited depth (<2 m)
Profile				
Length of part 1, L_1 (m)	5.000	1.693	5.000	3.415
Length of part 2, L_2 (m)	10.000	13.307	10.000	11.585
Diameter of part 1, D_1 (m)	0.500	1.349	0.500	1.632
Diameter of part 2, D_2 (m)	0.500	0.932	0.500	0.846
Pre-hole depth, H_{pre} (m)	–	–	2.150	1.260
Total length, $L_1 + L_2$ (m)	15.0	15.0	15.0	15.0
Total volume, V_{tot} (m^3)	2.945	11.498	2.945	13.656
Structural behaviour				
Maximum shear force at $d_0 = 50$ mm, Q_{max} (kN)	168.5	2021.1	162.1	2740.3
Maximum bend moment at $d_0 = 50$ mm, M_{max} (kN·m)	–	4732.7	232.0	8363.5
Maximum stress in concrete, σ_c (MPa)	16.02	19.83	19.83	19.83
Maximum strain in concrete, ϵ_c (%)	0.11	0.35	0.35	0.35
Maximum stress in reinforcement, σ_s (MPa)	396.37	413.87	416.24	414.62
Maximum strain in reinforcement, ϵ_s (%)	0.62	2.09	2.28	2.15

design solutions for pile construction reach nearly the same flexibility to lateral displacements and stress level (in concrete and reinforcement) in the pile head. Although the profile with varying sections has a much higher reduction in volume, the construction technique appears more difficult. For the uniform pile section with pre-holes, less work is necessary. However, the maintenance and durability problem on the material filling the pre-hole around the pile require more research.

Overall, the proposed design optimization shows a competitive approach and optimized solutions in pile design through structural optimization that can assure pile displacement capacity for super-long integral abutment bridges.

5.6. *Pile optimized design for large displacement*

From the above optimization procedures, the optimized piles could reach the displacement capacity approximately 30 mm for the Isola della Scala Bridge. However, for super-long integral abutment bridges that might be longer than the Isola della Scala Bridge, the thermal induced displacement would be larger. According to common design guidelines for bridges, it is assumed that the thermal induced strains ($\epsilon = \Delta L/L = \alpha\ \Delta T$) on the superstructure would exceed 20×10^{-5}. Hence, if the superstructure length reaches 500 m, the corresponding displacement on one bridge end would be 50 mm.

Therefore, the optimization procedure was also tried to determine the optimal (R/C) pile shapes subjected to the imposed lateral displacement of 50 mm on the pile head. Considering the abutment-pile connections, even if the pile is not required to resist the bending moment, the connections should be of sufficient lateral stiffness, rotational stiffness and bearing strength (Ahn et al., 2011). Furthermore, if a semi-integral abutment is applied, the pinned abutment-pile connection would dramatically increase the displacement

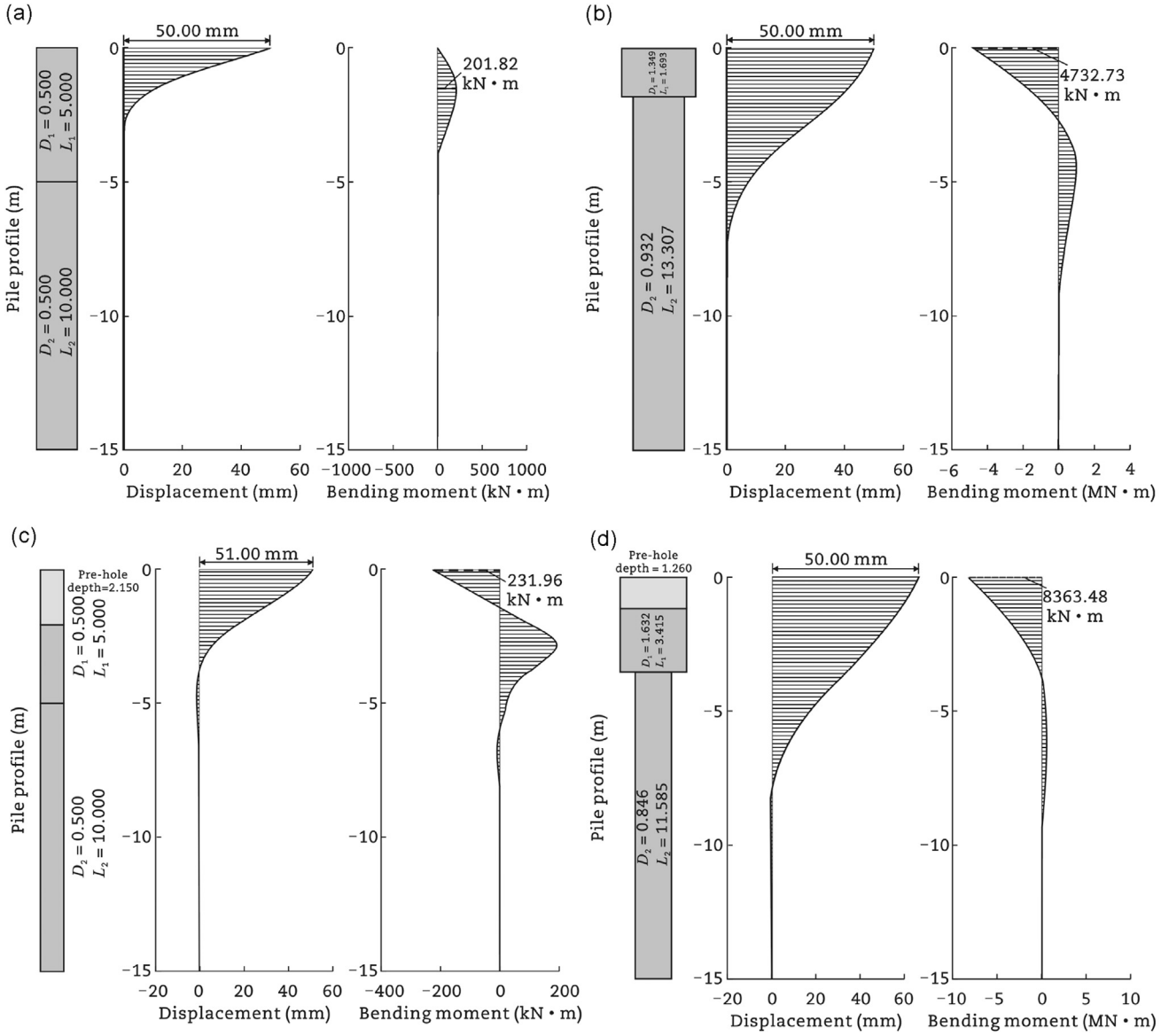

Fig. 15 – Optimized profile of R/C pile for imposed lateral displacement of 50 mm. (a) Pinned pile head without pre-hole. (b) Fixed pile head without pre-hole. (c) Fixed pile head with pre-hole of any depth. (d) Fixed pile head with pre-hole of limited depth.

capacity of the piles as observed and analysed (Dicleli and Albhaisi, 2004). Considering the same conditions as the Isola della Scala Bridge, four pile design optimization cases were considered as follow.

a) pinned pile head without a pre-hole (pinned head/no pre-hole).
b) fixed pile head without a pre-hole (fixed head/no pre-hole).
c) fixed pile head with a pre-hole of any depth (fixed head/pre-hole any depth).
d) fixed pile head with a pre-hole of limited depth (<2 m) with enough embedded length of the friction pile (fixed head/pre-hole limited depth < 2 m).

With the same objectives of total pile volume, constraints of total pile length of 15 m, minimum section diameter of 0.5 m (pre-hole depth limit of 2 m for case d), ultimate strain of concrete of 0.35% and 6.75% for steel, the obtained optimized pile profiles are listed in Table 8 and shown in Fig. 15.

As shown by the optimization results, the pinned head pile was the only case in which the material ultimate strains were not reached, thus proving a higher pile displacement capacity with the semi-integral abutment than with an integral abutment. Additionally, pre-holes evidently increase the displacement capacity of a fixed-head pile. If the pre-hole depth is not limited, the lateral displacement is limited by the optimized pile profile, and the required displacement capacity is reached; if the pre-hole depth is limited by pile embedment length requirements or for construction technique reasons, the high displacement capacity could still be reached with an optimized pile profile.

6. Conclusions

The following conclusions can be drawn within the limitations of the research presented in this paper.

(1) The current pile design optimization shows that laterally loaded piles could be optimized for better performance with less material; piles in integral abutment bridges require better performance for accommodating large lateral displacement. Therefore, an optimization procedure was proposed.
(2) The proposed optimization procedure for laterally loaded piles associates a finite element analysis (implemented in OpenSees) of the pile with an optimization algorithm (implemented in MATLAB) by suitably transferring data from the optimization algorithm to the FEM code and vice versa.
(3) The optimization procedure has been validated by first comparing the results with those obtained through a different optimization procedure available in the literature and carried out on a pile with same load and boundary conditions.
(4) By properly defining the objectives, constraints and design variables of the optimization problem, the piles could be optimized under different conditions through the procedure proposed, including a pile profile with two varying sections and a profile with a uniform section and pre-hole treatment. Different interactions between different soils (even layered) and piles are shown to be properly taken into account by linear and nonlinear springs simulating the soil and implemented in OpenSees.
(5) Through the design optimization procedure proposed, the piles could be designed with less materials and more displacement capacity, even if a reasonable and acceptable increase of stress levels occurs.
(6) The proposed design optimization procedure shows a competitive approach to the design of laterally loaded piles, with both material savings and sufficient rotational and displacement capacities for long integral abutment bridges.

Acknowledgments

The research was supported by the Recruitment Program of Global Experts Foundation (Grant No. TM2012-27), National Natural Science Foundation of China (Grant No. 51778148 and 51508103) and Fujian Provincial Education Department Research Foundation for Young Teacher (Grant No. JA150743). The authors would also like to acknowledge the Sustainable and Innovative Bridge Engineering Research Center (SIBERC) of the College of Civil Engineering, Fuzhou University (Fuzhou, China), and the Department of Civil Engineering, Environmental Engineering and Architecture of University of Cagliari (Cagliari, Italy).

REFERENCES

Adriaenssens, S., Block, P., Veenendaal, D., et al., 2014. Shell Structures for Architecture: Form Finding and Optimizatio. Routledge, London.
Ahn, J.H., Yoon, J.H., Kim, J.H., et al., 2011. Evaluation on the behavior of abutment–pile connection in integral abutment bridge. Journal of Constructional Steel Research 67 (7), 1134–1148.
Allahdadian, S., Boroomand, B., 2010. Design and retrofitting of structures under transient dynamic loads by a topology optimization scheme. In: The 3rd International Conference on Seismic Retrofitting, Iranian North-West Retrofitting Center (Iranian Retrofitting Researchers Ins.), Tabriz, 2010.
American Petroleum Institute (API), 2000. Recommended Practice for Planning, Designing, and Constructing Fixed Offshore Platforms: Working Stress Design. RP 2A-WSD. API Publishing Services, Washington DC.
Arockiasamy, M., Sivakumar, M., 2005. Effects of restraint moments in integral abutment bridges. In: 2005 FHWA Conference: Integral Abutment and Jointless Bridges, Baltimore, 2005.
Arsoy, S., Barker, R.M., Duncan, J.M., 1999. The Behavior of Integral Abutment Bridges. FHWA/VTRC 00-CR3. Virginia Transportation Research Council, Charlottesville.
Baptiste, K.T., Kim, W., Jeffrey, A., 2011. Parametric study and length limitations for prestressed concrete girder integral abutment bridges. Structural Engineering International (SEI) 21 (2), 151–156.
Boulanger, R.W., Curras, C.J., Kutter, B.L., et al., 1999. Seismic soil-pile-structure interaction experiments and analyses. Journal of Geotechnical and Geoenvironmental Engineering 125 (9), 750–759.
Briseghella, B., Zordan, T., 2007. Integral abutment bridge concept applied to the rehabilitation of a simply supported prestressed conventional concrete superstructure. Structural Concrete 8 (1), 25–33.

Briseghella, B., Fenu, L., Feng, Y., et al., 2013a. Topology optimization of bridges supported by a concrete shell. Structural Engineering International 23 (3), 285–294.
Briseghella, B., Fenu, L., Lan, C., et al., 2013b. Application of topological optimization to bridge design. Journal of Bridge Engineering 18 (8), 790–800.
Briseghella, B., Zordan, T., 2015. An innovative steel-concrete joint for integral abutment bridges. Journal of Traffic and Transportation Engineering (English Edition) 2 (4), 209–222.
Briseghella, B., Fenu, L., Feng, Y., et al., 2016. Optimization indexes to identify the optimal design solution. Journal of Bridge Engineering 21 (3), 04015067.
Burke Jr., M.P., 1993. Integral bridges: attributes and limitations. Transportation Research Board 1393, 1–8.
Burke Jr., M.P., 2009. Integral and Semi-integral Bridges. Wiley-Blackwell, Oxford.
David, T.K., Forth, J.P., 2011. Modelling of soil structure interaction of integral abutment bridges. International Journal of Civil and Environment Engineering 5 (6), 645–650.
Dicleli, M., Albhaisi, S., 2004. Estimation of length limits for integral bridges built on clay. Journal of Bridge Engineering 9 (6), 572–581.
Dong, J.C., Chen, B.C., Zhuang, Y.Z., et al., 2014. Technical research on the seamlessness and continuity transformation of existing multi-span simply-supported hollow slab bridge. In: The 7th International Conference of Bridge Maintenance, Safety and Management, Shanghai, 2014.
Erhan, S., Dicleli, M., 2015. Comparative assessment of the seismic performance of integral and conventional bridges with respect to the differences at the abutments. Bulletin of Earthquake Engineering 13 (2), 653–677.
Fenu, L., Serra, M., 1995. Optimum design of beams surrounded by a winkler medium. Structural and Multidisciplinary Optimization 9 (2), 132–135.
Fenu, L., Madama, G., 2006. Laterally loaded R/C bored piles with minimum horizontal top displacement. In: The 2nd FIB Congress, Naples, 2006.
Fiore, A., Monaco, P., Raffaele, D., 2012. Viscoelastic behaviour of non-homogeneous variable-section beams with post-poned restraints. Computers and Concrete 9 (5), 375–392.
Fiore, A., Foti, D., Monaco, P., et al., 2013. An approximate solution for the rheological behavior of non-homogeneous structures changing the structural system during the construction process. Engineering Structures 46, 631–642.
Fiore, A., Marano, G.C., Greco, R., et al., 2016. Structural optimization of hollow-section steel trusses by differential evolution algorithm. International Journal of Steel Structures 16 (2), 411–423.
Franco, J.M., 1999. Design and Field Testing of Jointless Bridges (Master thesis). West Virginia University, Morgantown.
Gama, D., Almeida, J.F., 2014. Concrete integral abutment bridges with reinforced concrete piles. Structural Concrete 15 (3), 292–304.
Greco, R., Marano, G.C., Fiore, A., 2016. Performance–cost optimization of tuned mass damper under low-moderate seismic actions. Structural Design of Tall and Special Buildings 25 (18), 1103–1122.
Greco, R., Marano, G.C., 2016. Optimum design of viscous dissipative links in wall-frame systems. Structural Design of Tall and Special Buildings 25 (9), 412–428.
Greimann, L.F., Abendroth, R.E., Johnson, D.E., et al., 1987. Pile Design and Tests for Integral Abutment Bridges. Iowa DOT Project HR-273. Iowa State University, Ames.
Greimann, L.F., Yang, P.S., Wolde-Tinsae, A.M., 1986. Nonlinear analysis of integral abutment bridges. Journal of Structural Engineering 112 (10), 2263–2280.
Horvath, J.S., 2004. Integral-abutment bridges: a complex soil-structure interaction challenge. In: 2004 Geotechnical Engineering for Transportation Projects, Los Angeles, 2004.
Huang, X., Xie, Y., 2008. Topology optimization of nonlinear structures under displacement loading. Engineering Structures 30 (7), 2057–2068.
Mahesh, T., 2005. Integral Bridges: the Final Frontier, Current and Future Trends in Bridge Design, Construction and Maintenance. Thomas Telford, London.
Marano, G.C., Trentadue, F., Petrone, F., 2014. Optimal arch shape solution under static vertical loads. Acta Mechanica 225 (3), 679–686.
MathWorks Inc., 2011. MATLAB-Product Documentation. Available at: http://www.mathworks.com/help/techdoc/. (Accessed 1 September 2016).
Matlock, H., 1970. Correlations for design of laterally loaded piles in soft clay. In: The 2nd Annual Offshore Technology Conference, Houston, 1970.
McGann, C.R., Arduino, P., 2011. Aterally-loaded Pile Foundation. Available at: http://opensees.berkeley.edu/wiki/index.php/Laterally-Loaded_Pile_Foundation. (Accessed 1 September 2016).
McGann, C.R., Arduino, P., Mackenzie-Helnwein, P., 2011. Applicability of conventional *p*-*y* relations to the analysis of piles in laterally spreading soil. Journal of Geotechnical and Geoenvironmental Engineering 137 (6), 557–567.
Menegotto, M., Pinto, P.E., 1973. Method of analysis for cyclically loaded reinforced concrete plane frames including changes in geometry and non-elastic behavior of elements under combined normal force and bending. In: International Association of Bridge and Structural Engineering (IABSE) Symposium of Resistance and Ultimate Deformability of Structures Acted on by Well-defined Repeated Loads, Lisbon, 1973.
Mosher, R.L., 1984. Load Transfer Criteria for Numerical Analysis of Axial Loaded Piles in Sand. Part 1: Load-transfer Criteria. US Army Engineering Waterways Experimental Station, Vicksburg.
Neves, M., Rodrigues, H., Guedes, J., 1995. Generalized topology design of structures with a buckling load criterion. Structural and Multidisciplinary Optimization 10 (2), 71–78.
OpenSees, 2011. The Open System for Earthquake Engineering Simulation. Available at: http://opensees.berkeley.edu. (Accessed 1 September 2016).
Quaranta, G., Fiore, A., Marano, G.C., 2014. Optimum design of prestressed concrete beams using constrained differential evolution algorithm. Structural and Multidisciplinary Optimization 49 (3), 441–453.
Reese, L.C., O'Neill, M.W., 1987. Drilled Shafts: Construction Procedures and Design Methods. FHWA-HI-88–8042. U.S. Department of Transportation, Washington DC.
Stromberg, L.L., Beghini, A., Baker, W.F., et al., 2010. Application of layout and topology optimization using pattern gradation for the conceptual design of buildings. Structural and Multidisciplinary Optimization 43 (2), 165–180.
Suykens, J.A.K., Vandewalle, J., De Moor, B., 2001. Intelligence and cooperative search by coupled local minimizers. International Journal of Bifurcation and Chaos 11 (8), 2133–2144.
Thanasattayawibul, N., 2006. Curved Integral Abutment Bridges (PhD thesis). University of Maryland, College Park, College Park.
Teughels, A., De Roeck, G., Suykens, J.A.K., 2003. Global optimization by coupled local minimizers and its application to FE model updating. Computers & Structures 81 (24–25), 2337–2351.
Vijayvergiya, V.N., 1977. Load-movement characteristics of piles. In: Ports 77 Conference, ASCE, New York, 1977.
Wasserman, E.P., 2007. Integral abutment design (practices in the United States). In: The 1st U.S. -Italy Seismic Bridge Workshop, Pavia, 2007.
Xue, J.Q., Briseghella, B., Chen, B.C., et al., 2014. Italian national road authority IABs strategy. In: The 7th International Conference of Bridge Maintenance, Safety and Management, Shanghai, 2014.
Yannotti, A., Sreenivas, A., White, L., 2005. New York State department of transportation's experience with integral

abutment bridges. In: 2005 FHWA Conference: Integral Abutment and Jointless Bridges, Baltimore, 2005.
Zordan, T., Briseghella, B., Mazzarolo, E., 2010. Structural optimization through step-by-step evolutionary process. Structural Engineering International 20 (1), 72–78.
Zordan, T., Briseghella, B., 2007. Attainment of an integral abutment bridge through the refurbishment of a simply supported structure. Structural Engineering International 17 (3), 228–234.
Zordan, T., Briseghella, B., Lan, C., 2011a. Parametric and pushover analyses on integral abutment bridge. Engineering Structures 33 (2), 502–515.
Zordan, T., Briseghella, B., Lan, C., 2011b. Analytical formulation for limit length of integral abutment bridges. Structural Engineering International 21 (3), 304–310.

Dr. Bruno Briseghella is distinguished professor and dean of the College of Civil Engineering, Fuzhou University, China, and founding director of the "Sustainable and Innovative Engineering Research Center". He graduated with a bachelor's and master's degree from Padova University, Italy, and a PhD from Trento University, Italy. His main research activities have been focused on bridge and structural design, integral abutment bridges, monitoring and retrofit of bridges, earthquake engineering and composite steel-concrete structures, both from the theoretical and experimental point of view.

Dr. Luigi Fenu graduated with master's degree in civil engineering from University of Cagliari, Italy, where he teaches structural design and is a researcher in this field. After starting his research in the field of foundation structures, now his main field of interest includes conceptual design (especially of innovative bridges) and structural optimization, together with the dynamic behaviour of materials, and the seismic behaviour of adobe buildings. He has a research fellowship at the SIBERC (Sustainable and Innovative Bridge Engineering Research Center) in Fuzhou University (China), where he is carrying out his studies on innovative curved bridges.

Dr. Junqing Xue is assistant researcher at the College of Civil Engineering, Fuzhou University (Fuzhou, China). He received his PhD in civil engineering from Trento University, Italy, in 2013. His research interests include jointless bridges, retrofit of existing bridges, composite steel and concrete structures.